Theor. Comput. Fluid Dyn. (2016) 30:511–527
DOI 10.1007/s00162-016-0395-8

ORIGINAL ARTICLE

M. E. Boghosian · K. W. Cassel

On the origins of vortex shedding in two-dimensional incompressible flows

Received: 30 April 2015 / Accepted: 14 April 2016 / Published online: 26 April 2016

Abstract An exegesis of a novel mechanism leading to vortex splitting and subsequent shedding that is valid for two-dimensional incompressible, inviscid or viscous, and external or internal or wall-bounded flows, is detailed in this research. The mechanism, termed the vortex shedding mechanism (VSM) is simple and intuitive, requiring only two coincident conditions in the flow: (1) the existence of a location with zero momentum and (2) the presence of a net force having a positive divergence. Numerical solutions of several model problems illustrate causality of the VSM. Moreover, the VSM criteria is proved to be a necessary and sufficient condition for a vortex splitting event in any two-dimensional, incompressible flow. The VSM is shown to exist in several canonical problems including the external flow past a circular cylinder. Suppression of the von Kármán vortex street is demonstrated for Reynolds numbers of 100 and 400 by mitigating the VSM.

Keywords Vortex splitting · Vortex shedding · Vortex shedding mechanism · Von Kármán vortex street

1 Introduction

A number of hypotheses regarding the origins of vortex splitting and subsequent shedding for inviscid/viscous and internal/external flows have been put forth. A popular explanation is that vortex shedding originates from an instability in the flow. Consequently, it is quite common to see vortex shedding interpreted as a result of a "Kelvin–Helmholtz-like" instability of the shear layer. Other explanations for the phenomenon include: (a) topological flow changes inside a recirculation region [1], (b) an eruption of secondary near-wall vorticity bisecting the main recirculation region [2], (c) a local absolute instability near the center of the recirculation region [3], (d) a global instability [4,5], and (e) vortex pinch-off due to exceeding a maximum value of circulation based on the Kelvin–Benjamin variational principle [6]; see the summary in Boghosian [7]. While the role of flow instabilities as *one* cause of the vortex splitting and shedding phenomenon is not questioned, the details of *how*, *when*, and *where* such an instability or other initiating cause can lead to vortex splitting and shedding needs further elucidation.

Previous research by Boghosian and Cassel [8] has indicated that pressure gradient forces having a specific magnitude signature (adverse, zero, and favorable in the streamwise direction) acting on regions in the flow having zero momentum play a critical role in making the physical link between the presence of an instability, for example, and the subsequent vortex splitting and shedding [8]. This scenario has been described as the pressure gradient mechanism (PGM). Essentially, the vortex or recirculation region is pulled apart by the adverse and favorable pressure gradients on upstream and downstream sides of the splitting point, respectively. The PGM may explain how the steady vortex structures observed by Theofilis et al. [1] evolve into an unsteady state.

Communicated by Dr. Jeff D. Eldredge.

M. E. Boghosian (✉) · K. W. Cassel
Mechanical, Materials and Aerospace Engineering Department, Illinois Institute of Technology, Chicago, IL, USA
E-mail: boghmic@iit.edu

This study aims to expand on the previous investigation of the PGM's role in vortex splitting and shedding [8]. First, by including viscous and body forces and eliminating directional dependence, the PGM is generalized into what is termed the vortex shedding mechanism (VSM), and secondly by offering a mathematical proof of the VSM that is valid for any two-dimensional, incompressible flow.

In this study, a vortex is defined to be a coherent, rotating flow structure, and a recirculation region is a similar structure resulting from flow separation that is present at a wall. However, the VSM acts on both structures in the same manner and the terms are interchangeable here. Vortex shedding is a process by which the vortex or recirculation region splits into two distinct vortical structures, with the downstream vortex being advected with the flow. In this investigation, vortex splitting is considered in scenarios in which the surface does not play a central role in the splitting process. That is, a surface may be essential to the initial formation of the vortex or recirculation region, but it is not required by the VSM for splitting or shedding.

The paper focuses on the splitting aspect of the shedding process and is organized as follows. In Sect. 2, a mathematical proof of the VSM is given that is valid for any two-dimensional, incompressible flow. The VSM is applied to an example vortex flow in Sect. 3. In Sect. 4, causality of the VSM is demonstrated from the numerical solutions of several model problems. In Sect. 5, it is shown that the VSM is present in the canonical problem of the external flow past a circular cylinder. Results are presented here on the ability to suppress the von Kármán vortex street via mitigation of the VSM, thereby illustrating that the VSM is a necessary condition for splitting and subsequent shedding. A summary and discussion of the relation of the VSM to the viscous-based finite Reynolds number vorticity ejection mechanism for vortex splitting and boundary layer separation follows in Sect. 6.

2 The vortex shedding mechanism

Consider a two-dimensional, incompressible flow in which a vortex or recirculation region is present. With respect to the splitting mechanism, the global flow field is considered to be quasi-steady, i.e., the vortex splitting event resulting from the VSM or PGM occurs on a much faster timescale than the evolution of the bulk flow. Numerical data from various simulations support the assertion that these two timescales are sufficiently distinct. For example, for the two-dimensional flow in a 75 % constricted channel at a Reynolds number of 400, there is more than an order of magnitude difference between the VSM and bulk flow timescales. Similar results are obtained for the two-dimensional flow past a circular cylinder at a Reynolds number of 100.

The following proof invokes the Q-criterion, a popular criterion originally put forth by Hunt et al. [9] for vortex identification. A vortex or recirculation region exists when $Q > 0$. In the analysis below, the Q-criterion is always evaluated at the center of an existing vortex or recirculation region. The initial vortex has by definition, $Q > 0$. We allow the existing vortex to be perturbed, either naturally due to an instability or forced via source terms. The Q-criterion is then re-evaluated after the disturbance. It is shown that several possible outcomes are possible depending on the sign of Q. If $Q < 0$ locally, then a saddle point must have occurred and the vortex experienced a splitting into two distinct structures. If Q remains positive after the flow disturbance, then the existing vortex (or recirculation region) is preserved. The section following the proof expresses the mathematically based VSM criteria from a Navier–Stokes perspective.

2.1 VSM: proof

The velocity gradient tensor, $\nabla \mathbf{v}$, can be decomposed using the Stokes–Cauchy decomposition into the symmetric rate-of-strain tensor, $\mathbf{S}$, and skew-symmetric rate-of-rotation, or vorticity, tensor, $\mathbf{R}$, as follows

$$\nabla \mathbf{v} = \mathbf{S} + \mathbf{R} \tag{1}$$

In two dimensions

$$\mathbf{S}(x, y) = \begin{bmatrix} \dfrac{\partial u}{\partial x} & \dfrac{1}{2}\left(\dfrac{\partial u}{\partial y} + \dfrac{\partial v}{\partial x}\right) \\ \dfrac{1}{2}\left(\dfrac{\partial u}{\partial y} + \dfrac{\partial v}{\partial x}\right) & \dfrac{\partial v}{\partial y} \end{bmatrix},$$

and

$$\mathbf{R}(x, y) = \begin{bmatrix} 0 & \frac{1}{2}\left(\frac{\partial u}{\partial y} - \frac{\partial v}{\partial x}\right) \\ \frac{1}{2}\left(\frac{\partial v}{\partial x} - \frac{\partial u}{\partial y}\right) & 0 \end{bmatrix}.$$

The velocity gradient tensor has the following characteristic equation

$$\lambda_i^2 + P\lambda_i + Q = 0, \tag{2}$$

where λ_i are the eigenvalues of $\nabla\mathbf{v}$. The first and second invariants of the velocity gradient tensor are, respectively,

$$P = -\text{tr}\,(\nabla\mathbf{v}) = -\left(\frac{\partial u}{\partial x} + \frac{\partial v}{\partial y}\right) = 0, \tag{3}$$

and

$$Q = \frac{1}{2}\left(\|\mathbf{S}\|^2 - \|\mathbf{R}\|^2\right) = \frac{\partial u}{\partial x}\frac{\partial v}{\partial y} - \frac{\partial u}{\partial y}\frac{\partial v}{\partial x}. \tag{4}$$

Note that the first invariant, P, is identically zero by the continuity equation for an incompressible fluid. The second invariant, Q, is used as a criterion for vortex identification. A vortex is defined when $Q > 0$ and a local pressure minimum exists. It is noted that for two-dimensional incompressible flows, the Q-criterion and λ_2-criterion are the same [10,11].

The second invariant, Eq. (4), expressed in terms of the streamfunction, $\psi(x, y)$, is

$$Q = \frac{\partial^2\psi}{\partial x^2}\frac{\partial^2\psi}{\partial y^2} - \left(\frac{\partial^2\psi}{\partial x\partial y}\right)^2, \tag{5}$$

where

$$u = \frac{\partial\psi}{\partial y} \quad \text{and} \quad v = -\frac{\partial\psi}{\partial x}. \tag{6}$$

Let $\psi(x, y)$ be a function with continuous partial derivatives that has a local critical point at (x_0, y_0). At a critical point in the streamfunction, the first derivatives are

$$\frac{\partial\psi}{\partial x}(x_0, y_0) = 0, \tag{7}$$

$$\frac{\partial\psi}{\partial y}(x_0, y_0) = 0. \tag{8}$$

The critical point supplies a necessary condition on the streamfunction for a vortex splitting.

The *Hessian* matrix of the streamfunction is

$$\mathbf{H}(x, y) = \begin{bmatrix} \frac{\partial^2\psi}{\partial x^2} & \frac{\partial^2\psi}{\partial x\partial y} \\ \frac{\partial^2\psi}{\partial x\partial y} & \frac{\partial^2\psi}{\partial y^2} \end{bmatrix}.$$

Note that because derivatives are continuous, the order of differentiation with respect to x and y can be interchanged. The determinant of the Hessian matrix is

$$|\mathbf{H}| = \frac{\partial^2\psi}{\partial x^2}\frac{\partial^2\psi}{\partial y^2} - \left(\frac{\partial^2\psi}{\partial x\partial y}\right)^2, \tag{9}$$

which from Eq. (5), shows that

$$Q = |\mathbf{H}|. \tag{10}$$

Therefore, for a two-dimensional, incompressible fluid, the determinant of the Hessian matrix for the streamfunction is equal to the second invariant of the velocity gradient tensor.

The second partial derivative test (SPDT) for a function of two variables provides a qualitative description of the behavior of the streamfunction at the critical point and is used to provide a sufficiency condition for a vortex splitting event. This test asserts that a critical point is:

(i) a local minimum if:

$$Q(x_0, y_0) > 0 \quad \text{and} \quad \frac{\partial^2 \psi}{\partial r^2}(x_0, y_0) > 0, \tag{11}$$

(ii) a local maximum if:

$$Q(x_0, y_0) > 0 \quad \text{and} \quad \frac{\partial^2 \psi}{\partial r^2}(x_0, y_0) < 0, \tag{12}$$

(iii) a saddle point if:

$$Q(x_0, y_0) < 0, \tag{13}$$

(iv) inconclusive if:

$$Q(x_0, y_0) = 0, \tag{14}$$

where r in parts (i) and (ii) can represent either spatial direction x or y.

From the above SPDT, if $Q > 0$, the sign of rotation determines if there is a local minimum (i) or maximum (ii) in the streamfunction at the center of the vortex. If an existing vortex having $Q > 0$ undergoes a splitting event such that there are two new distinct vortices, then each of the new vortices require $Q > 0$ separated by a point or region in the flow where $Q < 0$, i.e., there is a saddle in the streamfunction field. Mathematically, the VSM states:

Given a two-dimensional incompressible flow, an existing vortex or recirculation region will undergo a splitting event at a location, if and only if (1) there is a critical point in the streamfunction, $\partial\psi/\partial x = \partial\psi/\partial y = 0$, and (2) the determinant of the Hessian matrix, or equivalently the Q-criterion, are locally less than zero, i.e. $|H| = Q < 0$.

The above proof shows that the two requirements for the VSM are both necessary and sufficient. Figure 1 illustrates the local topological changes in the streamfunction that an elliptically shaped vortex experiences as Q varies from positive (vortex) to negative (splitting). From results of numerical simulations presented in the following sections, it is observed that at the *onset* of vortex splitting, *all* invariants of the velocity gradient tensor are zero, i.e. $P = Q = 0$. As a result, all eigenvalues of the characteristic Eq. (2) are zero. Also, if $Q = 0$, then by Eq. (4), the magnitude of the rate-of-strain-rate tensor, $\|\mathbf{S}\|^2$, equals the magnitude of the rotation-rate tensor, $\|\mathbf{R}\|^2$.

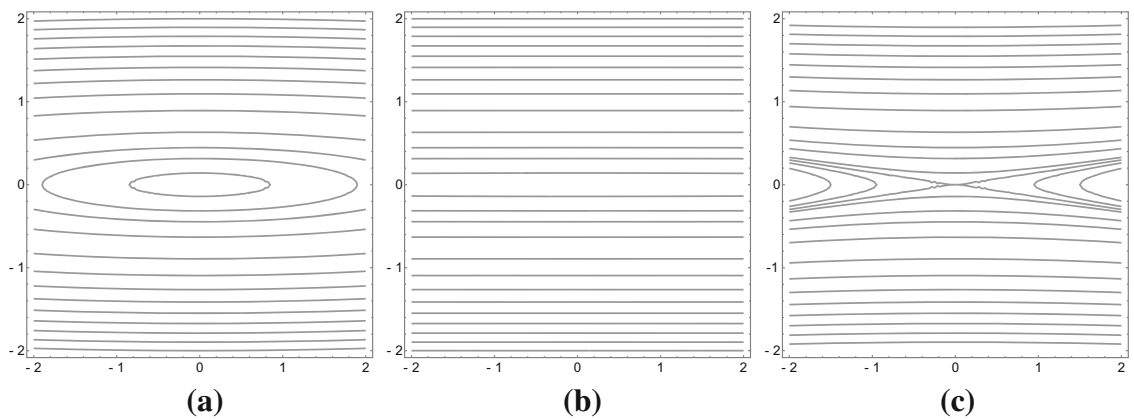

Fig. 1 Evolution of an elliptically shaped vortex as a function of the second invariant, Q, in the neighborhood of a critical point at (0, 0), where $\partial\psi/\partial x = \partial\psi/\partial y = 0$. **a** $Q > 0$, SPDT Case (i) or (ii). **b** $Q \approx 0$, SPDT Case (iv). **c** $Q < 0$, SPDT Case (iii)

2.2 VSM: a Navier–Stokes perspective

An equation for the pressure of an incompressible flow is derived by taking the divergence of the Navier–Stokes equations and using continuity to simplify the result. This results in a Poisson equation for pressure

$$\nabla^2 p = 2\left(\frac{\partial u}{\partial x}\frac{\partial v}{\partial y} - \frac{\partial u}{\partial y}\frac{\partial v}{\partial x}\right) + \nabla \cdot \mathbf{f}_b, \tag{15}$$

where $\mathbf{f}_b$ is the body force. Comparing Eqs. (4) and (15) shows that

$$Q = -\frac{1}{2}\left(\nabla \cdot \mathbf{f}_b - \nabla^2 p\right). \tag{16}$$

Next, let the RHS of the Navier–Stokes equations, i.e., the forces, be written as

$$\mathbf{f}_{\text{net}} = -\nabla p + \frac{1}{Re}\nabla^2 \mathbf{v} + \mathbf{f}_{\text{b}}. \tag{17}$$

Note that by including both body forces and viscous effects, the VSM generalizes the previously identified PGM [8]. In addition, the directional dependence on x or y in the PGM is now eliminated. Taking the divergence of the net force, $\nabla \cdot \mathbf{f}_{\text{net}}$, gives

$$\nabla \cdot \mathbf{f}_{\text{net}} = -\nabla^2 p + \frac{1}{Re}\nabla^2(\nabla \cdot \mathbf{v}) + \nabla \cdot \mathbf{f}_{\text{b}}. \tag{18}$$

If the fluid is incompressible, the divergence of the viscous terms is identically zero by continuity, and

$$\nabla \cdot \mathbf{f}_{\text{net}} = -\nabla^2 p + \nabla \cdot \mathbf{f}_{\text{b}}. \tag{19}$$

Comparing Eqs. (16) and (19), observe that the divergence of the net force is related to the Q-criterion according to

$$Q = -\frac{1}{2}\nabla \cdot \mathbf{f}_{\text{net}}. \tag{20}$$

Therefore, the criteria for a vortex splitting, $Q < 0$ at a critical point of $\psi(x, y)$, becomes

$$\nabla \cdot \mathbf{f}_{\text{net}} > 0. \tag{21}$$

Using Eq. (6), the critical point occurs at a location where

$$u = 0, \tag{22}$$
$$v = 0. \tag{23}$$

Thus, the critical point is a location of *zero* fluid momentum. From a Navier–Stokes perspective, the VSM states:

Given a two-dimensional incompressible flow, an existing vortex or recirculation region will undergo a splitting event at a location, if and only if, it is a location of zero momentum, $u = v = 0$, and the divergence of the net forces is greater than zero, i.e. $\nabla \cdot \mathbf{f}_{\text{net}} > 0$.

Physically, the VSM can be interpreted as follows. When a vortex or recirculation region undergoes a splitting into two distinct structures, there is a negative force accelerating motion to the left and a positive force accelerating motion to the right of the splitting location, essentially pulling the vortex or recirculation region apart at the zero momentum location. A force distribution can significantly affect an existing flow structure where and when there is no existing fluid momentum to overcome, i.e., where the momentum is zero. In contrast, a divergence of the net force less than zero yields forces acting in "compression" in all directions on the vortex such that the structure is preserved in this state.

2.3 VSM: reduced form (PGM)

The RHS of the Navier–Stokes equations, $\mathbf{f}_{\text{net}}$, is the sum of the pressure gradient, body, and viscous forces. From the above proof, vortex splitting will occur when $Q < 0$ at the critical point where $u = v = 0$. If there are no body forces, then by Eq. (19) we have a reduced form of the VSM, denoted as the Pressure Gradient Mechanism (PGM), where

$$\nabla \cdot \mathbf{f}_{\text{net}} = -\nabla^2 p. \tag{24}$$

Equation (21) is used to provide the criterion for the PGM as

$$\nabla^2 p < 0. \tag{25}$$

Physically, this is interpreted as follows. When a vortex or recirculation region undergoes a splitting into two distinct structures, there is only an adverse pressure gradient acting to the left and a favorable pressure gradient to the right of the zero momentum point (for bulk flow from left to right), essentially pulling the vortex or recirculation region apart.

3 Elliptically shaped vortex example

Although vortices and recirculation regions have different origins, they behave in the same manner with regard to their splitting and shedding. As a result, the study of these flow structures can be performed using a simple flow environment consisting of an initially steady solution for an elliptically shaped vortex. Note that this elliptically shaped vortex is not the elliptic vortex as defined in Batchelor [12]. It will be shown analytically that the elliptically shaped vortex can experience vortex splitting and shedding via the VSM.

Consider an elliptically shaped vortex as the steady base flow in an infinite domain defined by

$$u(y) = \frac{\alpha}{b^2} y, \quad v(x) = -\frac{\alpha}{a^2} x, \quad p(x, y) = \frac{\alpha^2}{2a^2 b^2}(x^2 + y^2), \tag{26}$$

where u and v are the velocity components in x and y, respectively, and p is the pressure. The parameter α represents the strength of the pressure gradient due to the vortex, and its sign determines the direction of rotation. The parameters a and b are constants that, together with α, set the geometry of the vortex or recirculation region. A circular vortex is obtained when $a = b$. The elliptically shaped vortex as defined above satisfies the steady, incompressible Navier–Stokes equations. Also, observe that the momentum is zero, i.e. $u = v = 0$, at the center of the vortex, which is at the origin $(x, y) = (0, 0)$. Thus, the base flow contains the first requirement of the two necessary conditions for the VSM to produce a splitting event. Because the center of the vortex is the region of interest, the infinite velocities far from the center of the vortex are of no consequence.

For the base flow defined by Eq. (26), the viscous terms are identically zero throughout the domain and there is no body force. In the VSM, viscous effects simply retard the existing motion and do not play a central role in the splitting process. Thus, the pressure gradient force is the only force contribution to the net force in the base flow. An analysis is performed next to determine an estimate of what expansion force is required to split the elliptically shaped vortex.

First, evaluate the divergence of the net force field in the base flow as follows

$$\nabla \cdot \mathbf{f}_{\text{net}} = -\nabla^2 p = -\frac{\partial^2 p}{\partial x^2} - \frac{\partial^2 p}{\partial y^2} = -\frac{2\alpha^2}{a^2 b^2} < 0. \tag{27}$$

Observe that this is negative for all a, b, and α, i.e. for any vortex shape, strength, or direction of rotation. This reflects the fact that an existing vortex or recirculation region, with no other forces acting on it, is a structure that resists splitting and shedding. Thus, something must occur in the flow that will overcome this inherent resistance. In other words, an expansion force superimposed on the flow must overcome the resistance that exists due to the existing compressive pressure gradient field.

Let us imagine a body force acting in the x-direction of the form

$$\mathbf{f}_{\text{b}} = f_x(x, y)\mathbf{i} + 0\mathbf{j} \tag{28}$$

that is superimposed on the base flow. The net force acting on the zero momentum region at the center of the vortex must have a positive divergence in order to cause a local expansion and lead to splitting of the vortex according to

$$\nabla \cdot \mathbf{f}_{\text{net}} = -\nabla^2 p + \nabla \cdot \mathbf{f}_{\text{b}} > 0 \tag{29}$$

in the vicinity of the zero momentum point at $(x, y) = (0, 0)$. Hence, substituting $\mathbf{f}_{\text{b}}$ from Eq. (28) into Eq. (29) gives

$$\frac{\mathrm{d}f_x}{\mathrm{d}x} > \nabla^2 p. \tag{30}$$

The above equation implies that a body force distribution is required such that the divergence (expansion) of the net force is sufficient to overcome the convergence (compression) due to the pressure field. This is illustrated in Fig. 1c for the elliptically shaped vortex, and numerical confirmation of the VSM is provided in the following sections for additional canonical problems.

It is noted that the addition of a body force perturbation changes the flow and pressure fields. Therefore, direct application of Eq. (30) with Eq. (27) may not be possible, because Eq. (27) is based on the flow field prior to the application of the body force.

4 Causality

In this section, cause (net force magnitude having a positive divergence acting on the zero momentum location) and effect (vortex splitting and shedding) is demonstrated through numerical experiments on several simple model flow problems. Two-dimensional, steady base flows (elliptically shaped vortex and constricted channel) are perturbed using the body force term, $\mathbf{f}_{\text{b}}$, in the x-momentum equation. The resulting flow behavior is then observed numerically.

All subsequent results are found from integrating the unsteady, two-dimensional, incompressible, Navier–Stokes equations. The spectral-element code, Nek5000, developed and maintained by the Argonne National Laboratory is used for all simulations performed in this research [13]. The number of spectral elements is typically 2000. High resolution is achieved both with tenth-order polynomials in space and third-order temporal accuracy. The number of degrees of freedom in two dimensions is at least 2×10^5 for the model problems in this section and approaches 1×10^6 for the canonical case in the next section.

A post-processing tool is illustrated in this section that can identify a potential splitting and shedding event. This diagnostic tool consists of a superposition of three contour plots. The first plot is the streamfunction, the second is of the divergence of the net force, $\nabla \cdot \mathbf{f}_{\text{net}}$, and the third is a plot of zero momentum locations $(u = v = 0)$. The diagnostic tool is demonstrated here and in the following sections, e.g., see Fig. 2c.

4.1 Elliptically shaped vortex

Consider an initially elliptically shaped vortex defined by Eq. (26) and as shown in Fig. 2a that contains a location of zero momentum at the center of the vortex, i.e, the origin. The domain is $-10 < x < 10$ and $-10 < y < 10$. The steady solution for $Re = 500$ is found and used as the initial condition in a restarted simulation where a perturbation is introduced. The base flow is defined by initial and inlet boundary conditions from Eq. (26) with $a = 12$ and $b = \alpha = 1$. The upper and lower boundaries at $y = \pm 10$ are modeled as moving walls with $u = y$, $v = 0$, and $p = (x^2 + y^2)/2$. A perturbation is imposed via the body force, $\mathbf{f}_{\text{b}} = f_x(x, y)\mathbf{i} + 0\mathbf{j}$, in the x-momentum equation centered at $(x, y) = (0, 0)$ according to

$$f_x(x, y) = -\gamma \ \sin(x) \ \exp\left[-\left(\frac{x-x_0}{\sigma_x}\right)^2\right] \ \exp\left[-\left(\frac{y-y_0}{\sigma_y}\right)^2\right] \tag{31}$$

to see if the vortex can be split according to the VSM. Here, $\sigma_x = \sigma_y = 1.0$, $x_0 = y_0 = 0$, and γ is a parameter representing the amplitude of the perturbation. The Gaussian distribution allows the perturbation to be focused in the vicinity of the origin. The perturbation is initiated at a nondimensional time of $t = 0.001$ and removed at a time of $t = 100.0$. If the perturbation is removed, the solution eventually returns to the elliptically shaped vortex.

Figure 2 shows the effect of the perturbation on the elliptically shaped vortex. Part *a* of this figure shows the original elliptically shaped vortex before the body force perturbation is applied. The zero momentum location

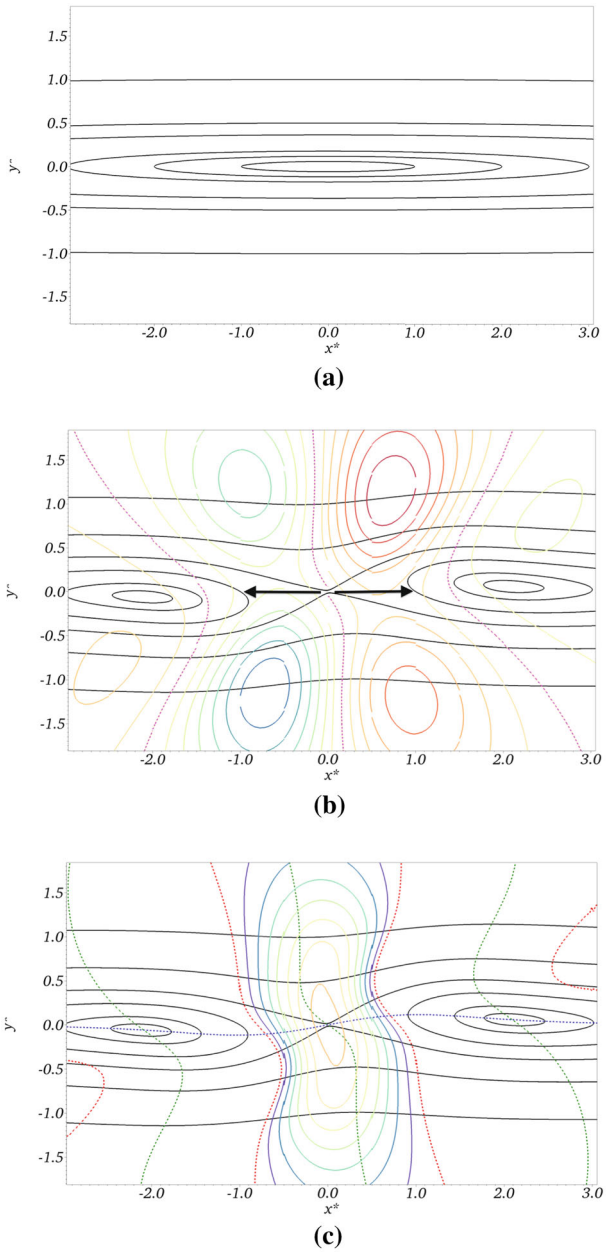

Fig. 2 Elliptically shaped vortex splitting due to the VSM. **a** Streamfunction contours of initial elliptically shaped vortex. **b** Split vortex. $\mathbf{f}_{\text{net}}$ and streamfunction contours. Signature of $(-, 0, +)$ is present near origin. *Pink dashed lines* denote $\mathbf{f}_{\text{net}} = 0$. **c** $\nabla \cdot \mathbf{f}_{\text{net}}$ and streamfunction contours. Positive values of $\nabla \cdot \mathbf{f}_{\text{net}} > 0$ are in color and *dashed red lines* denotes its zero contour. Zero momentum location shown by intersection of $u = 0$ (*blue dashed line*) and $v = 0$ (*green dashed line*)

is at the center of the vortex. The entire flow field contains a negative divergence per Eq. (27) prior to splitting. In part (b), observe that the initial elliptically shaped vortex has split into two vortices centered near the origin with $\gamma = 1$ when the body force (31) is applied. Here, the net force has the signature of $(-, 0, +)$. A negative, or retarding, force is present in a vertical region where $x < 0$ and a positive or accelerating force exists in a vertical band where $x > 0$, essentially pulling the vortex apart in the x-direction. The dashed pink line denotes $\mathbf{f}_{\text{net}} = 0$. Part (c) of this figure shows the divergence of the net force contours superimposed on the streamfunction contours. A region of positive divergence (colored contours) surrounds the origin containing zero momentum (green and blue dashed lines). A zero value of divergence is denoted by a red dashed line. Observe that the splitting location is surrounded by a positive divergence acting on a zero momentum location as required by the VSM.

The diagnostic post-processing tool illustrated in part (c) can be a helpful way to observe when and where a vortex splitting may occur. Simply track the above contours over time and observe the dynamics of the zero momentum location with respect to the positive divergence of the net force.

This elliptically shaped vortex example explicitly shows how the net force having the magnitude signature of $(-, 0, +)$ corresponding to a positive divergence acts on zero momentum fluid to *cause* vortex splitting i.e.the VSM.

4.2 Constricted planar channel

A steady solution for the *internal* flow in a two-dimensional constricted channel at a Reynolds number of 100 is used as the initial condition in a restarted simulation. In the restarted case, a perturbation is initiated after a time of approximately 0.005 using the body force. The requirements of the VSM, a magnitude signature of $(-, 0, +)$ on the net force having a positive divergence, is again achieved through the addition of a body force per Eq. (31); however, the $\sin(x)$ factor is removed. Here, $\gamma = -1$, $\sigma_x = 1$, $\sigma_y = 1$, $x_o = \pi$, and $y_o = -0.7$. The Gaussian distribution allows for the splitting to be localized at the point (x_o, y_o). Therefore, splitting of the recirculation region near the lower wall is considered in this example. Figure 3a shows the streamfunction contours after the perturbation but before splitting has occurred. The flow contains two locations of zero momentum ($u = v = 0$) near the centers of the recirculation regions where the dashed blue and green lines intersect. A future third location of zero momentum is developing near $x = 4$ at the end of the lower recirculation region.

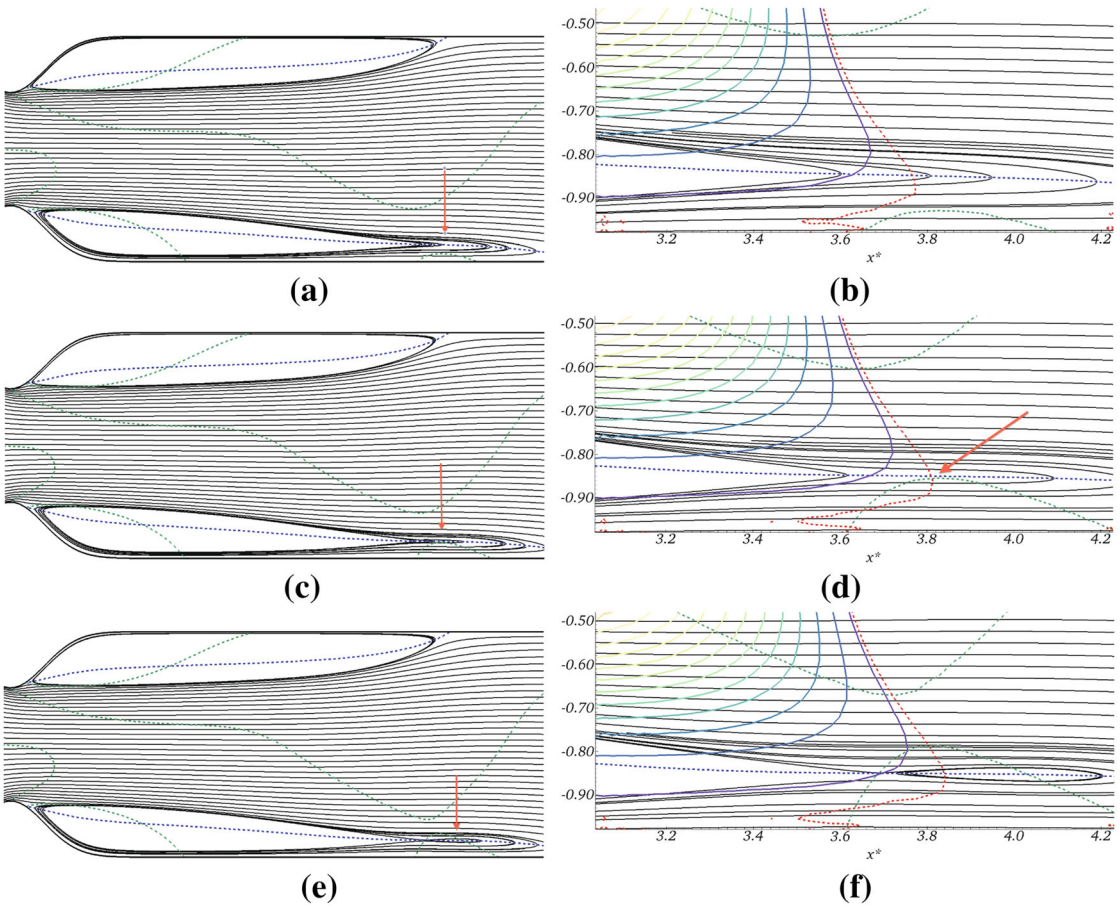

Fig. 3 Example of a forced (due to body force perturbation) splitting in a planar channel at $Re = 100$ with a 50 % constriction; splitting occurs when $\nabla \cdot \mathbf{f}_{\text{net}} > 0$ (contours shown by *solid colored lines*) coincide with zero momentum locations ($u = 0$ *dashed blue line*, $v = 0$ *dashed green line*). **a** Before splitting. **b** Before splitting. $\nabla \cdot \mathbf{f}_{\text{net}} < 0$; **c** Onset of splitting; **d** Onset of splitting. $\nabla \cdot \mathbf{f}_{\text{net}} \approx 0$; **e** After splitting; **f** After splitting. $\nabla \cdot \mathbf{f}_{\text{net}} > 0$

The effect of the body force perturbation on the streamfunction contours can be seen in Fig. 3b at a time very near the onset of splitting of the lower-wall recirculation region. In part (b), contours of $\nabla \cdot \mathbf{f}_{\text{net}} > 0$ are superimposed on the streamfunction for the case of pre-splitting. Again, zero momentum regions are shown by intersecting blue and green dashed lines. A region of zero momentum is about to form near $x = 3.8$. The zero contour of $\nabla \cdot \mathbf{f}_{\text{net}}$ is shown by a red dashed line in parts (b), (d), and (f). At the onset of splitting, the zero momentum location just intersects the positive divergence region as shown in part (d). A timestep later, the recirculation region locally splits into two structures owing to the positive divergence producing a decelerating force acting on the left and an accelerating force acting to the right of the zero momentum point. The post-splitting flow field is shown in parts (e) and (f) of the figure. As the solution evolves, the downstream recirculation region advects with the bulk flow, i.e., shedding. Note that there are other regions with a positive divergence of the net force; however, these regions are not superimposed on zero momentum locations, and the vortex does not undergo a splitting at those locations.

In this same geometry, but at a Reynolds number of 400 with a 75 % constriction, splitting and shedding occurs naturally, i.e., no body force perturbation is necessary. Instead, the perturbation is supplied by a "convective-like" instability that produces a spatially growing pressure wave in the shear layers emanating from the constriction [8]. This case is shown in Fig. 4. Here, the PGM-based splitting and shedding is a special case of the VSM. Tracking points A and B in parts (a) to (c) of this figure illustrates the PGM. In part (a), the PGM has become applicable at points A and B. The upper recirculation region has already split at point B and is at the onset of splitting at points A and C as shown in part (b) of Fig. 4. Part (c) shows the flow immediately after splitting at point A.

The two examples in this section show that the resulting net force, having the specific magnitude signature of $(-, 0, +)$ corresponding to a positive divergence, acts on zero momentum locations to *cause* vortex splitting and subsequent shedding. Thus, causality of the VSM is demonstrated by these numerical experiments. The converse is also true, a positive divergence of the net force cannot cause vortex or recirculation region splitting in flows if there are no locations of zero momentum.

5 Flow past a circular cylinder

5.1 Vortex shedding mechanism

Vortex splitting and shedding due to the PGM was first revealed in the problem of flow in an internal constricted channel by Boghosian and Cassel [8]. In this section, the presence of the VSM is demonstrated to occur naturally, i.e., without external perturbation, in the canonical problem of the two-dimensional *external* flow past a circular cylinder at a Reynolds number of $Re = 100$. This Reynolds number is above the critical value of $Re = 47$ for unsteady vortex shedding, and the simulations here reveal the expected von Kármán vortex street.

Figure 5 shows instantaneous streamlines indicating the start of vortex shedding in the near wake of the cylinder. Parts (a), (c), and (e) show streamfunction contours illustrating the sequence prior to splitting, at onset of splitting, and after splitting, respectively. The VSM is observed to occur in parts (b), (d), and (f) where the focus is on the splitting location. Here, a zero momentum location occurs where $u = 0$ (blue dashed line) intersects $v = 0$ (green dashed line). Positive values of the divergence are shown in color and the zero value by a dashed red line. Note in part (b) that there is no zero momentum point as the $u = 0$ and $v = 0$ contours are approaching each other but do not intersect. In part (d), these contours are about to intersect indicating the onset of splitting. From part (f), it is observed that splitting occurs when the positive divergence contour coincides with the zero momentum location. Therefore, the VSM is shown to be present at this location.

Figure 6 shows the von Kármán vortex street starting to develop over a larger region behind the cylinder compared to the previous figure, which only shows the initial splitting. Regions of positive divergence of the net force are shown shaded. The zero contour of divergence is indicated by a solid red line. Zero momentum locations are shown by dashed blue lines ($u = 0$) and dashed green lines ($v = 0$). Part (a), at an arbitrary time defined as t_1, shows a pre-split recirculation region in the lower half of the near wake. However, here a point of zero momentum is not yet present as the contours of $u = 0$ and $v = 0$ do not coincide. In parts (b) and (c), observe that the lower recirculation region undergoes a splitting between a time of $t_1 + 0.45$ and $t_1 + 1.075$ as the positive divergence of the net force intersects the zero momentum location. The recirculation region is then shed between $t_1 + 1.075$ and $t_1 + 5.4$ as shown in parts (c) and (d). The next stage of splitting for the developing von Kármán vortex street is shown in parts (e) and (f). Here, the upper recirculation region is split between $t_1 + 6.125$ and $t_1 + 6.6$ due to the intersection of zero momentum and positive divergence

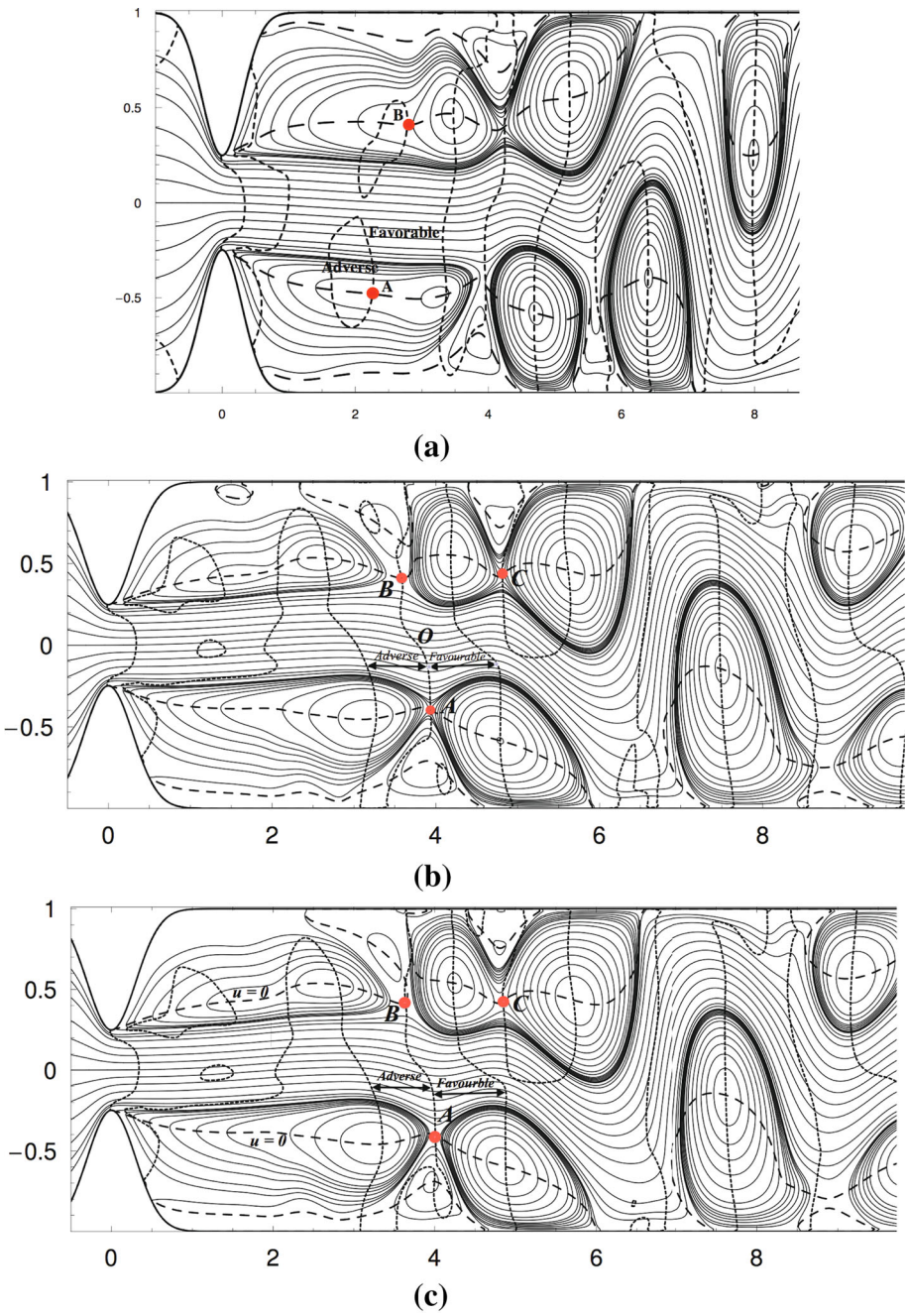

Fig. 4 Example of shedding in a planar channel at $Re = 400$ with a 75 % constriction [8]. Case is unforced, i.e., no body force perturbation. Tracking points A and B (*red dots*) in time illustrates the PGM. Short *dashed black lines* denote $\partial p/\partial x = 0$ contours and longer *dashed lines* indicate the $u = 0$ contour. **a** Early recirculation region development, $t = 5.2$. **b** Prior to lower recirculation region shedding, $t = 8.2$. **c** After lower recirculation region shedding, $t = 8.3$

contours. This figure shows that the VSM is clearly present in the von Kármán vortex street. Although not shown here, the pressure gradient field in the near wake is composed of a spatially growing wave, reminiscent of a convective-like instability similar to the constricted channel problem [8].

The primary finding in this section is that the von Kármán vortex street results from the VSM operating in the near wake. Here, the net force field that induces the splitting may derive from convective, absolute, global, or Föppl instabilities. Recall that the VSM provides the details linking the divergence of the net force field (cause) to the vortex shedding (effect).

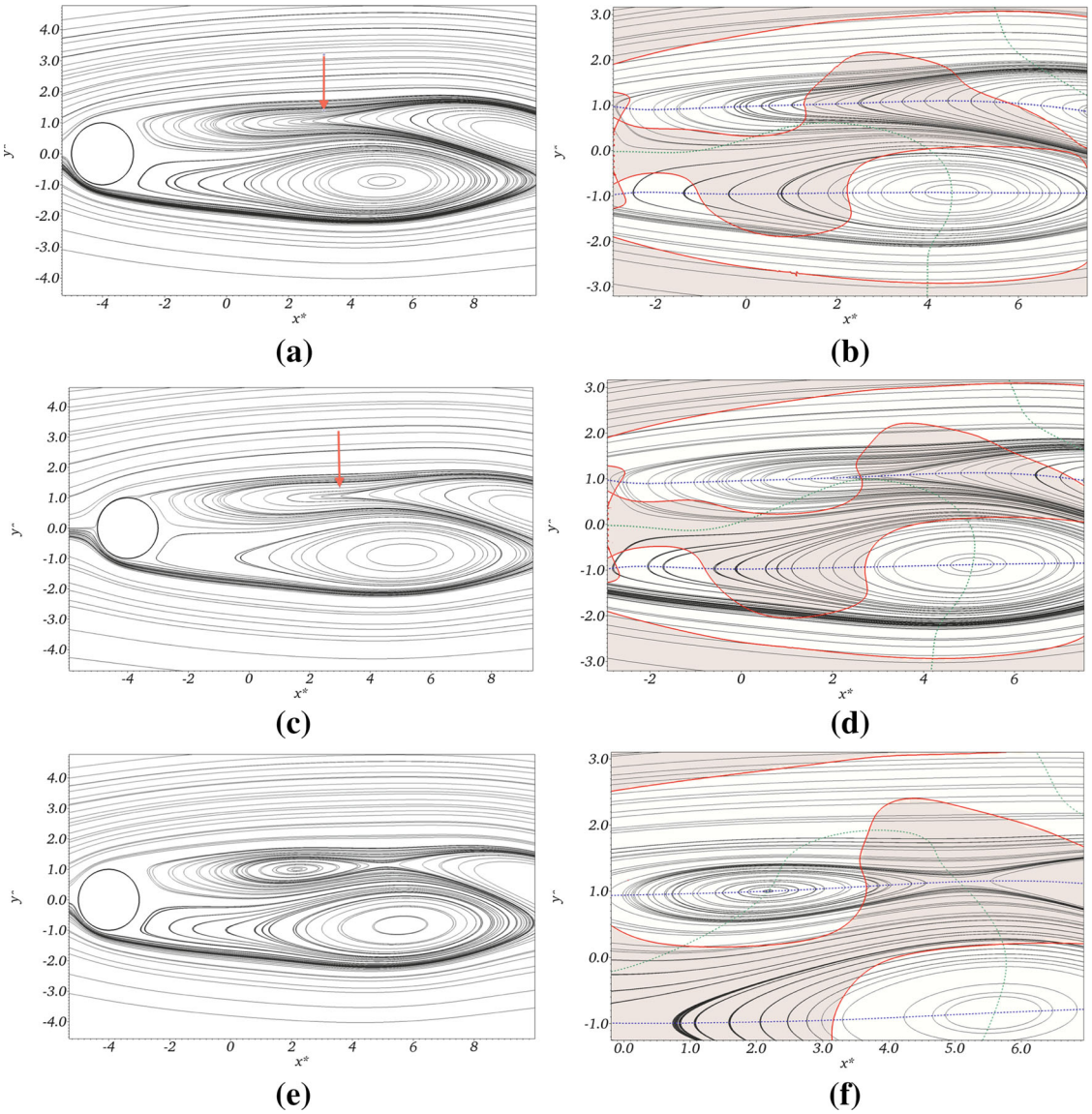

Fig. 5 The external flow past a circular cylinder at $Re = 100$ (near-field) illustrating the VSM for the first splitting; contours of instantaneous streamlines (*solid black lines*), $\nabla \cdot \mathbf{f}_{\text{net}} > 0$ (*colored lines*), $\nabla \cdot \mathbf{f}_{\text{net}} = 0$ (*dash red line*), and zero momentum ($u = 0$ *dashed blue line*, $v = 0$ *dashed green line*). **a** Pre-split. **b** Pre-split (zoom). **c** Onset of splitting. **d** Onset of splitting (zoom). **e** Post-split. **f** Post-split (zoom)

5.2 Suppression of the von Kármán vortex street

The VSM is found to occur naturally in the external flow past a circular cylinder as shown in the previous section. However, if the two criteria of the VSM truly comprise a necessary and sufficient condition, then removal of one of these would suppress vortex splitting and shedding. Two Reynolds numbers, $Re = 100$ and $Re = 400$, are considered.

The body force term is again used as a tool to modify the net force in a local region behind the cylinder. The functional form of the x-momentum body force, $\mathbf{f_b}$, in both cases is given by

$$\mathbf{f}_{\text{b}}(x, y) = \gamma \ \exp^{\left[-\left(\frac{x-x_0}{\sigma_x}\right)^2\right]} \ \exp^{\left[-\left(\frac{y-y_0}{\sigma_y}\right)^2\right]} \mathbf{i} + 0\mathbf{j}, \tag{32}$$

where $x_0 = -3.0$, $y_0 = 0$, $\sigma_x = 2.0$, and $\sigma_y = 1.0$ for both cases. This is similar to Eq. (31); however, here the $\sin(x)$ factor is removed. Because the splitting location changes spatially over time, finding an acceptable

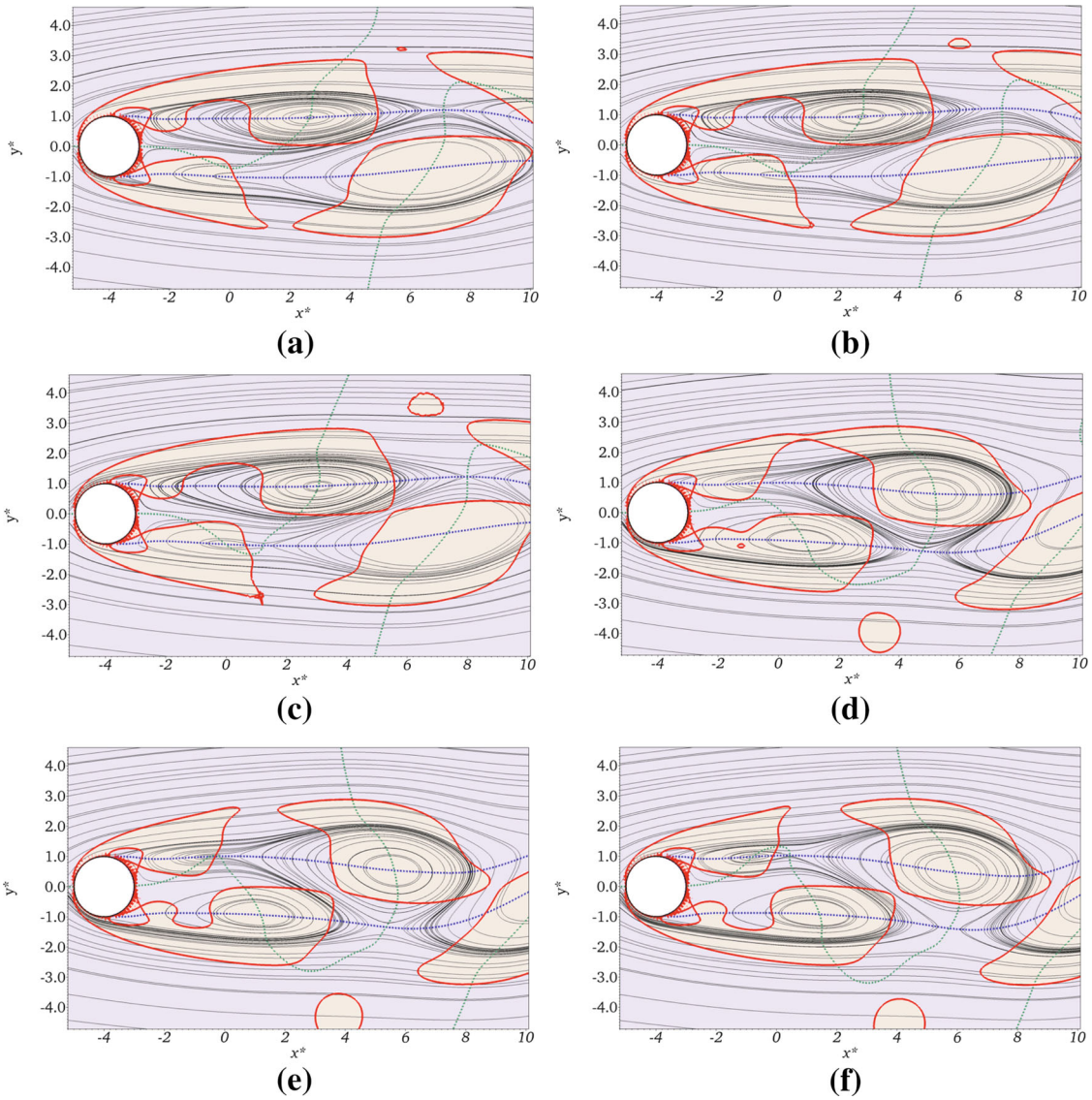

Fig. 6 The external flow past a circular cylinder for $Re = 100$ (far-field) and start of the von Kármán vortex street; contours of instantaneous streamlines (*solid black lines*), $\nabla \cdot \mathbf{f}_{\text{net}} > 0$ (tan region), $\nabla \cdot \mathbf{f}_{\text{net}} = 0$ (*dashed red line*), and zero momentum (intersection of *dashed blue*, $u = 0$, and *green lines*, $v = 0$) illustrate the presence of the VSM. **a** t_1. **b** $t_1 + 0.45$. **c** $t_1 + 1.075$. **d** $t_1 + 5.4$. **e** $t_1 + 6.125$. **f** $t_1 + 6.60$

amplitude, γ, using the methods of Sect. 4 may only provide an initial estimate of the required magnitude. The intention here is simply to demonstrate the importance of the VSM in this problem by showing that when it is eliminated, no shedding occurs. No control theory or sophisticated strategy is involved in the vortex suppression. An amplitude of $\gamma = -0.5$ is used for the lower Reynolds number case. It is noted that an amplitude value of -0.2 did not suppress vortex shedding in the case with $Re = 100$. For the larger Reynolds number case of $Re = 400$, an amplitude of $\gamma = -3.0$ is used. In these two cases, the value of γ in the body force term is specified to be negative resulting in a positive divergence of the net force that mitigates the naturally occurring negative divergence.

The results of the simulations shown in Fig. 7 demonstrate that vortex shedding is indeed suppressed through the use of an imposed body force in both cases. Parts (a) and (b) show the streamfunction contours after addition of the highly localized body force. Flow separation still occurs immediately behind the cylinder in a limited region; however, there is no vortex splitting and shedding or subsequent von Kármán vortex street in either case, and the solution is time independent. The corresponding vorticity contours are shown in parts

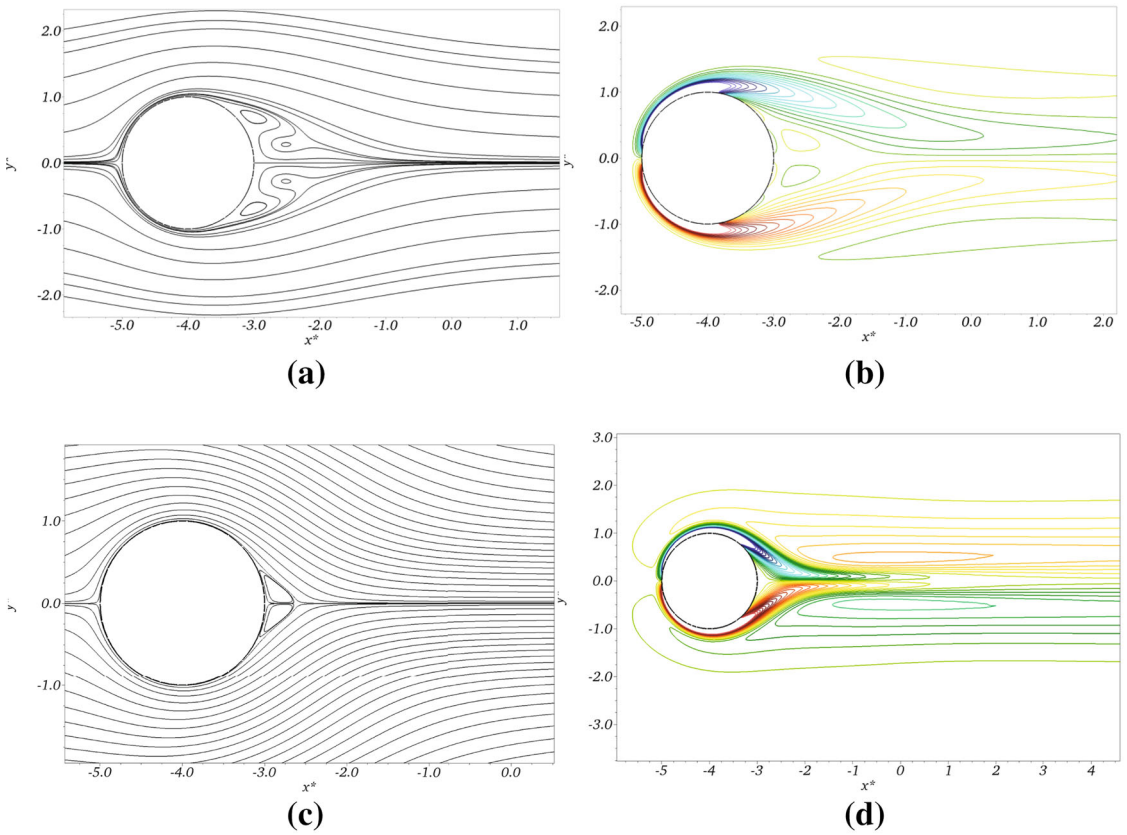

Fig. 7 Suppression of the von Kármán vortex street via mitigation of the VSM (solution is time independent for both Reynolds numbers). **a** Streamfunction contours for $Re = 100$. **b** Vorticity contours for $Re = 100$. **c** Streamfunction contours for $Re = 400$. **d** Vorticity contours for $Re = 400$

(b) and (d) of this figure. Here, the shear layers are observed to be constrained near the symmetry line. With the larger magnitude body force used in the $Re = 400$ case, smaller stationary recirculation regions behind the cylinder are observed with an even greater constraint on the shear layer near the symmetry line. In this case, a less conservative value of γ could have been used; however, our aim is simply to show that elimination of the VSM eliminates the von Kármán vortex street, not to find the critical threshold value for control.

In suppressing vortex shedding with the VSM, each problem will have its own critical value of γ depending on the existing local pressure gradient field that is to be modified. Determining the critical γ for vortex shedding suppression would be valuable from a practical point of view in a control setting; however, this is very difficult in the wake of a cylinder owing to the advection of the eventual splitting location with the local flow field. This has been circumvented in the present approach by applying a Gaussian force distribution in the general vicinity of the splitting locations. Note that in all cases involving splitting mitigation, there are no instances for which the VSM is not satisfied but splitting still occurs. This is consistent with the necessary and sufficient conditions for the VSM as prescribed by the proof.

These two cases demonstrating suppression of vortex shedding support the hypothesis that the von Kármán vortex street is explained by the VSM acting in the near wake of the cylinder. That is, even though the instability that ultimately leads to vortex shedding is still present in the flow, mitigating the VSM provides a means to prevent formation of the von Kármán vortex street. In other words, the VSM is both a necessary and sufficient condition for vortex shedding regardless of the initiating mechanism, i.e., instability or otherwise.

6 Discussion

Two simple and intuitive, but quite general, mechanisms, termed the VSM and its special case, the PGM, describing vortex or recirculation region splitting and subsequent shedding, are detailed in this research.

Table 1 Summary of vortex or recirculation region splitting and shedding in several two-dimensional flows as a function of zero momentum and $\nabla \cdot \mathbf{f}_{\text{net}} > 0$

Flow	Zero momentum	$\nabla \cdot \mathbf{f}_{\text{net}} > 0$	Splitting
(1) Elliptically shaped vortex in an infinite domain			
$Re = 500$	Yes	No	No
$Re = 500$	Yes	Yes (imposed)	Yes
(2) Internal flow in a constricted channel			
$Re = 100$ with 50 % constriction	Yes	No	No
$Re = 100$ with 50 % constriction	Yes	Yes (imposed)	Yes
$Re = 400$ with 75 % constriction	Yes	Yes	Yes
(3) External flow past circular cylinder			
$Re = 100$	Yes	Yes	Yes
$Re = 100, 400$	Yes	No (imposed)	No
(4) External flow over forward-facing step			
$Re = 1000$	Yes	Yes	Yes

Both mechanisms are based on the presence of a specific magnitude signature $(-, 0, +)$ of the net force corresponding to a positive divergence of the force field acting on regions where the momentum is zero. The VSM is found to explain how, why, and where splitting and shedding of vortices and recirculation regions occur in a wide variety of two-dimensional, incompressible fluid dynamics problems, such as *external* flows (flow past a circular cylinder, flow past a forward-facing step, and an elliptically shaped vortex) and *internal* flows (flow in a constricted planar channel).

A mathematical proof of the VSM shows that the net force with a magnitude signature of $(-, 0, +)$ corresponding to a positive divergence acting on a location where the momentum is zero provides *necessary* and *sufficient* conditions for vortex or recirculation region splitting and shedding for any two-dimensional, incompressible flow. In addition, this proof shows that the PGM is a special case of the VSM in the absence of body forces. The vortex splitting and shedding criteria is found to be independent of: (1) Reynolds number, (2) problem geometry, and (3) source of the net force distribution, $\mathbf{f}_{\text{net}}$.

Table 1 summarizes the numerical results in this research relative to the VSM criteria. Note that results from the forward-facing step problem are consistent with the findings presented, but they are not shown. From the table, it can be seen that both the zero momentum region and the required force distribution are necessary for vortex splitting; cases without one or the other do not experience a splitting or shedding event, thereby demonstrating causality.

The origin of the net force that results in splitting by the VSM is not unique, i.e., it can originate from various sources such as instabilities, inherent nonlinearities in the Navier–Stokes equations, etc. One common source is spatially growing waves, e.g., "convective-like" instabilities. This instability is observed in the external flow past a backward-facing step [14], the external flow past a circular cylinder, the internal flow in a constricted channel [8], and in laminar separation bubbles with turbulent reattachment [15]. Whereas neither an instability nor the presence of a shear layer are necessary requirements for a vortex or recirculation region splitting and subsequent shedding event, shear layers are often present in problems with vortex shedding due to the existence of large velocity gradients. In addition, whereas viscous effects play an important role in the formation of shear layers, recirculation regions, and vortices, the viscous effects may play a lesser role in the splitting of these structures. If the flow can be treated as inviscid, then distinctions remain between the VSM and PGM. In the inviscid limit, the VSM retains the body force term and considers a generalized net force direction.

Just as it is possible to split vortices by imposing a positive force divergence in flows where they do not occur naturally, e.g., the elliptically shaped vortex, it is also possible to suppress shedding in scenarios in which the VSM occurs naturally by eliminating the positive force divergence at locations of zero momentum. Using insights from the VSM, suppression of the von Kármán vortex street is demonstrated. It is postulated that the success of various control strategies, such as surface suction/blowing, auxiliary control cylinders in the near wake, acoustic waves, and others, to suppress the vortex shedding phenomenon may in fact be a result of how these methods modify the pressure gradient or net force field. Further investigation of vortex shedding suppression via pressure gradients or net forces using optimal control theory is needed, and the present results suggest that one could target either the mechanism that produces $\mathbf{f}_{\text{net}}$, such as an instability, or the VSM itself.

A straightforward diagnostic tool is proposed that assists in anticipating if a vortex or recirculation region will undergo a splitting event. The tool consists of a superposition of three contour plots, (1) streamfunction,

(2) $u = v = 0$, and (3) positive divergence of the net force, the latter two corresponding directly to the VSM. These contours may be tracked in time, and splitting is expected when the $u = 0$ and $v = 0$ contours intersect the positive divergence region. It is also noted that the following are *zero* at the location of the *onset* of vortex splitting: (1) momentum, (2) $\nabla \cdot \mathbf{f}_{\text{net}}$, (3) Q-criterion, λ_2 and Δ-criterion, and (4) kinetic energy.

Recall that at the outset, the timescale on which the splitting process evolves is taken to be much faster than that of the overall bulk flow evolution. Note, however, that there could be flows where the timescale of the splitting is of the same order as the overall bulk flow field. In this case, there may be other splitting mechanisms present. However, at high Reynolds numbers, the timescales of the splitting and bulk flow are more likely to be distinct, and splitting resulting from the VSM more dominant.

The VSM requires an existing vortex or recirculation region to be present in the flow before a splitting can occur. By their nature, these flow structures have locations where the momentum is zero. If a moving frame of reference is chosen and the zero momentum location in the vortex or recirculation region no longer exists in the moving frame, then the VSM does not apply. Therefore, the VSM criteria only applies when the frame of reference is moving with the vortex center, and as such, it is not Galilean invariant.

Because the VSM can occur in vortices or recirculation regions at locations where the fluid momentum is zero, it is highly sensitive to external influences due to experimental noise or numerical disturbances. Specifically, it is possible, and maybe even likely, that noise or disturbances could lead to additional VSM occurrences on much smaller temporal and/or spatial scales than would occur in the underlying base flow. Therefore, "noisy" environments would likely lead to more complex splitting events than the VSM-induced splitting that is envisioned here. Ultimately, instabilities, nonlinearities, or noise can produce force distributions that can act upon locations in the flow where the fluid momentum is zero resulting in a splitting via the VSM.

The VSM appears to play a critical role in finite Reynolds number unsteady separation in some flows. Research by Obabko and Cassel [2,16] suggests an alternative viscous mechanism as a cause of high-Reynolds number shedding in wall-bounded shear flows subject to an adverse streamwise pressure gradient. For sufficiently large Reynolds numbers, the shedding process appears to be initiated by intermittent ejections of near-wall secondary vorticity having a "spike-like" character from within the boundary layer. Each boundary layer event ejects fluid away from the wall and splits the primary or parent recirculation region into discrete co-rotating vortices that are then shed with the flow. In this mechanism, a sufficiently large adverse pressure gradient acting along the surface is a necessary condition for an ejection event to occur within the boundary layer. Three Reynolds number regimes are identified: low, moderate, and high (i.e., limit as $Re \to \infty$). The critical Reynolds numbers for each regime are problem dependent.

We postulate that the VSM-based splitting and shedding of the primary vortex may be a *prerequisite* for an ejection spike of near-wall vorticity. For example, this eruption phenomenon is found to occur in the external flow past a circular cylinder at a Reynolds number of $Re = 9500$, see for example, Koumoutsakos and Leonard [17]. For this problem, the Reynolds number considered is in the moderate Reynolds number regime. From our simulations of this geometry for $Re = 9500$, an eruption event is visible at a time of approximately $t = 1.9$. A splitting of the primary recirculation region due to the VSM is observed to occur *prior* to and directly above the eruption location. It is possible that in these problems, a VSM-based vortex splitting and shedding may be a necessary precursor to the occurrence of a moderate Reynolds number regime eruption event by creating a "corridor" or pathway allowing for the release of the trapped boundary layer vorticity close to the surface. It is also possible that the eruption acts as the cause producing a pressure gradient field having the required signature of $(+, 0, -)$ that then initiates the VSM.

Because the viscous eruptive mechanism occurs in high-Reynolds number boundary layers, it raises the question as to whether the VSM can occur *naturally* (only being a consequence of the governing equations) in a boundary layer flow? The answer is no, the VSM cannot occur naturally in leading-order boundary layer theory. The VSM can only occur if one considers a special form of the inviscid outer flow's streamwise pressure gradient that is imposed on the boundary layer. This form must locally have the correct pressure gradient sign distribution of $(+, 0, -)$. However, the occurrence of the VSM here is due to *imposed* boundary conditions, and not directly from the governing equations. If, in the moderate Reynolds number regime, the VSM is proved to be a necessary prerequisite for the formation of a "spike" and ultimately an ejection of vorticity, then the absence of a naturally occurring VSM in non-interacting boundary layers would suggest that the finite Reynolds number "spike" and ejection of near-wall vorticity may *not* be the manifestation of the boundary layer eruption, i.e., the van Dommelen singularity [2]. This would have profound consequences for our understanding of high-Reynolds number, wall-bounded flows. Further research on determining the VSM's role in unsteady separation is ongoing.

Acknowledgments Research reported in this publication was supported by the National Institute of Diabetes and Digestive and Kidney Diseases (NIDDK) of the National Institutes of Health under Award Number R01DK090769. The content is solely the responsibility of the authors and does not necessarily represent the official views of the National Institutes of Health. In addition, the authors want to thank Dr. Aleksandr V. Obabko and Professor Sudhakar E. Nair for insightful discussions that improved this work.

References

1. Theofilis, V., Hein, S., Dallmann, U.: On the origins of unsteadiness and three-dimensionality in a laminar separation bubble. Philos. Trans. R. Soc. A **358**, 3229–3246 (2000)
2. Obabko, A., Cassel, K.: Navier–Stokes solutions of unsteady separation induced by a vortex. J. Fluid Mech. **465**, 99–130 (2002)
3. Marquillie, M., Ehrenstein, U.: On the onset of nonlinear oscillations in a separating boundary-layer flow. J. Fluid Mech. **490**, 169–188 (2003)
4. Ehrenstein, U., Gallaire, F.: Two-dimensional global low-frequency oscillations in a separating boundary-layer flow. J. Fluid Mech. **614**, 315–327 (2008)
5. Griffith, M., Leweke, T., Thompson, M., Hourigan, K.: Steady inlet flow in stenotic geometries: convective and absolute instabilities. J. Fluid Mech. **616**, 111–133 (2008)
6. Gharib, M., Rambod, E., Shariff, K.: A universal time scale for vortex ring formation. J. Fluid Mech. **360**, 121–140 (1998)
7. Boghosian, M.E.: Flow in partially constricted planar channels-origins of vortex shedding and global stability of Navier–Stokes solutions. Ph.D. thesis, Illinois Institute of Technology, Chicago, Illinois (2011)
8. Boghosian, M., Cassel, K.: A pressure-gradient mechanism for vortex shedding in constricted channels. Phys. Fluids **25**, 477–492 (2013). doi:10.1063/1.4841576
9. Hunt, J., Wray, A., Moin, P.: Eddies, stream, and convergence zones in turbulent flows. Center for Turbulence Research Report CTR-S88, pp. 193–208 (1988)
10. Kolar, V.: Vortex identification: new requirements and limitations. Int. J. Heat Fluid Flow **28**, 638–652 (2007)
11. Jeong, J., Hussain, F.: On the identification of a vortex. J. Fluid Mech. **285**, 69–94 (1995)
12. Batchelor, G.: Introduction to Fluid Dynamics. Cambridge University Press, Cambridge (1967)
13. Fischer, P.: An overlapping Schwarz method for spectral element solution of the incompressible Navier–Stokes equations. J. Comput. Phys. **133**, 84–101 (1997)
14. Kaiktsis, L., Karniadakis, G., Orszag, S.: Unsteadiness and convective instabilities in two-dimensional flow over a backward-facing step. J. Fluid Mech. **321**, 157–187 (1996)
15. Alam, M., Sandham, N.: Direct numerical simulation of short laminar separation bubbles with turbulent reattachment. J. Fluid Mech. **410**, 1–28 (2000)
16. Obabko, A., Cassel, K.: On the ejection-induced instability in Navier–Stokes solutions of unsteady separation. Philos. Trans. R. Soc. A **363**, 1189–1198 (2005)
17. Koumoutsakos, P., Leonard, A.: High-resolution simulations of the flow around an impulsively started cylinder using vortex methods. J. Fluid Mech. **296**, 1–38 (1995)